

Supplementary Data

MATERIAL AND METHODS

AAV vector design and production

Details of the design of the *RPGRco* (*RPGR* complementary DNA [cDNA]) and the rAAV2tYF-GRK1-*RPGRco* vector were described in a previous publication.^{S1} The *RPGRco* cDNA was codon optimized based on the human codon-usage frequency to increase the codon adaptation index (CAI) from 0.73 to 0.87 and the frequency of optimized codons from 32% to 57%. In addition, the unstable composition of the purine-rich repetitive sequence in the *ORF15* region of the *RPGR* gene was modified by increasing the GC content from 47.3% to 56.1% and decreasing the maximum repeat size from 50 bp to 17 bp. These changes are predicted to reduce the alternative splicing frequency, prolong the mRNA half-life, and stabilize the gene. The redesigned *RPGRco* encodes a full-length human RPGR protein and the 1152 amino acid sequence is identical to the National Center for Biotechnology Information (NCBI) reference sequence NP_001030025 and CCDS 35229.1.

The vector used in this study was produced using a recombinant herpes simplex virus (HSV) complementation system in suspension-cultured baby hamster kidney (sBHK) cells, as previously described.^{S2} The vehicle was the balanced salt solution (BSS, Alcon, Fort Worth, TX) containing 0.014% Tween-20.

Vector characterization

Vector concentration (vector genomes [vg]/mL), purity (silver-stained sodium dodecyl sulfate-polyacrylamide gel electrophoresis [SDS-PAGE] analysis), infectivity (tissue culture 50% infectious dose), sterility, and concentrations of endotoxin and HSV protein were measured as previously described.^{S3} Testing for mycoplasma, bacteria, and fungi was performed according to standard microbiological methods. Vector identity was confirmed by DNA sequencing, and pH measurement of the vector product was by standard laboratory methods. Results are provided in Supplementary Table S5. Concentrations of BHK protein, bovine serum albumin, benzoylserine, and AVB ligand were measured in drug substance by enzyme-linked immunosorbent assay (ELISA), using commercially available kits and HSV and BHK DNA were measured by quantitative PCR (qPCR) (data not shown).

Vector administration

Subretinal injections were performed in anesthetized animals as previously described.^{S4} Briefly, under direct visualization of a surgical microscope, an incision was made in the cornea using a 30-gauge micro vitreoretinal blade, and a 33-gauge blunt-tipped needle was inserted through the corneal incision toward the back of the eye while avoiding the lens and penetrating the neuroretina to reach the subretinal space. One microliter (1 μ L) of vector suspension or vehicle, each containing 0.1% fluorescein to allow confirmation of the injection location, was slowly injected subretinally while the retina was visualized to confirm successful dosing. If reflux of greater than 25% of the dosing volume occurred, as determined by the surgeon occurred, the animal was excluded from the study and replaced. Residual dosing formulations were frozen for later testing by qPCR to confirm the concentration of vector administered.

Ophthalmic examination

Masked ocular observations by the surgeon were made to evaluate complications from the injection procedure or bleeding within the first week. After review of the masked findings, extra animals were removed from the study by day 7.

Animals were observed daily for mortality and signs of illness. Body weights of each animal were obtained on the day of dosing, weekly thereafter, and on the day of scheduled sacrifice. Ophthalmic examinations, used to evaluate the eyes for signs of toxicity by slit lamp biomicroscopy and indirect ophthalmoscopy, were conducted during the week prior to scheduled sacrifice by a licensed veterinary ophthalmologist who was blinded to dose group. Abnormalities were described using standard terminology.

ERG

Scotopic and photopic ERG tests were performed on both eyes. Animals were dark adapted overnight (at least 10 h) before scotopic tests, which were performed with increasing light intensities of 25, 250, and 2500 mcDs/m². Ten responses at each intensity were recorded and averaged. Following scotopic measurement, the mice were light adapted for 5 min to a white background light of 30 cds/m². Photopic cone recordings were performed with in-

creasing flash intensities at 1.25, 5, 10, and 25 cds/m² in the presence of 30 cds/m² background light. Fifty responses at each intensity were recorded and averaged.

Clinical chemistry, histopathology, and immunohistochemistry

At sacrifice, blood for hematology (hemoglobin, hematocrit, neutrophils, lymphocytes, monocytes, eosinophils, basophils, red cell count, platelet count, and white cell count); clinical chemistry (ALT, AST, blood urea nitrogen, total protein, alkaline phosphatase, and albumin:globulin ratio); and serum for immunogenicity analysis (measurement of antibodies) were obtained. A complete external and internal examination was performed on all animals, including body orifices and cranial, thoracic, and abdominal organs and tissues. Brain, heart, liver, kidneys, spleen, thymus, lungs (with large bronchi), adrenals, and testes/ovaries were weighed. Sections of the following tissues were stained with hematoxylin and eosin and examined histologically: injected and uninjected eye with optic nerve, brain, liver, spleen, heart, lung, kidneys, parotid glands, testes/ovaries, and gross lesions. The following tissues were collected for potential histopathology: adrenal gland, cecum, colon, diaphragm, duodenum, epididymis, esophagus, femur with bone marrow, gallbladder, ileum, jejunum, lymph node, pancreas, sciatic nerve, pituitary, prostate, skeletal muscle, skin, stomach, thymus, thyroid/parathyroid gland, urinary bladder. Nonocular histology would be performed based on gross findings.

All gross findings from different organs were recorded in descriptive terms including locations(s), size, shape, color, consistency, and number. All eyes were collected into modified Davidson's solution and transferred to 10% neutral buffered formalin and processed for histopathology examination (hematoxylin and eosin staining). Sections of injected and uninjected eyes of 4 animals per group per termination time point were also prepared for RPGR immunohistochemical staining to document expression and subcellular localization of RPGR. Slides from vector-injected groups were evaluated in a masked fashion. Slides from vehicle control eyes were identified as such during slide reading.

Detection of antibodies to RPGR

Antibodies to RPGR in serum were evaluated by ELISA. Briefly, microtiter plates were coated with a truncated human RPGR protein consisting of N-terminal 399 amino acids and C-terminal 98

amino acids (Genscript Biotech, Piscataway, NJ) or mouse immunoglobulin (IgG; Sigma Aldrich, St. Louis, MO) and incubated overnight. Plates were washed and blocked, and then diluted mouse test serum was added. Customized mouse monoclonal anti-human RPGR antibody (clone 1F4D1; Genscript) was used as standard and positive control in the assay. After sample incubation, a cocktail of horseradish peroxidase-conjugated anti-mouse IgG was added to detect antibodies bound to RPGR. Tetramethyl benzidine substrate was then added and absorbance measured spectrophotometrically. A positive response was defined as an OD450 value higher than cut point 0.119 when the serum was diluted 1:50.

RPGR stability test

Stability of the codon-optimized *RPGR* was assessed by DNA sequencing, mRNA sequencing and protein proteomic analysis *in vitro* and *in vivo*. To test the DNA stability after subretinal injection *in vivo*, frozen retinal tissues from Rd9 mice after rAAV2tYF-GRK1-*RPGRco* administration were processed for DNA extraction using All-Prep DNA RNA Mini kit (Qiagen, Germantown, MD), according to the manufacturer's protocol. AAV vector genome sequences including the GRK1 promoter and *RPGRco* cDNA was amplified using Platinum PCR SuperMix High Fidelity (ThermoFisher Scientific, Grand Island, NY). The PCR products were then cleaned up using DNA Clean & ConcentratorTM-5 (Zymo Research, Irvine, CA) and sent for Sanger sequencing performed at Eurofins Genomics (Huntsville, AL). The Sanger sequencing reads were then assembled *de novo* using ContigExpress and aligned to a reference sequence using AlignX, both of which are components of Vector NTI software.

RPGRco mRNA transcribed from AAV vector was sequenced after reverse transcription. Briefly, retinal tissue from uninjected and vector-injected eyes were processed for RNA extraction (Qiagen, Germantown, MD) and the resulting total tissue RNA was used as template for reverse transcription followed by PCR amplification. The amplified PCR products were then sequenced, and all sequencing data were assembled based on the overlapping cDNA fragments using Vector NTI software, to generate a consensus sequence that was compared to the human *RPGRco* reference sequence for analysis.

Stability of vector-expressed RPGR protein was analyzed by Western blot and immunoprecipitation followed by liquid chromatography and mass spectrometry (LC-MS/MS). HEK293 cells trans-

ected with plasmid pTR-*RPGRco*, or retinal tissue from AAV vector-injected Rd9 mice, was homogenized in RIPA lysis buffer containing protease inhibitor. Whole cell/tissue lysate after protein quantification was separated on 4%–20% SDS-PAGE and transferred to a polyvinylidene fluoride membrane. After blocking with 5% nonfat dry milk for 1 h at room temperature, the membrane blots were incubated overnight at 4°C with the primary antibody (customized mouse monoclonal anti-human RPGR, clone 1F4D1, Genscript). After washing and reaction with secondary antibody (HRP-conjugated goat anti-mouse IgG; Jackson ImmunoResearch, West Grove, PA), the blots were developed for chemiluminescence detection and imaged using a digital camera (Chemidoc, Bio-Rad, Hercules, CA).

Whole lysate was also immunoprecipitated by anti-RPGR antibody and separated on SDS-PAGE and the gel was stained by Coomassie brilliant blue R-250. The RPGR bands were then excised for proteomic analysis. Briefly, the excised bands were digested with sequencing-grade endoproteases trypsin, chymotrypsin, and GluC using the manufacturer's recommended protocol (Promega, Madison WI). Nano-LC/MS/MS was performed using a Thermo Scientific Q Exactive HF Orbitrap mass spectrometer equipped with an EASY Spray nanospray source (ThermoFisher Scientific, Grand Island, NY) operated in positive ion mode. Se-

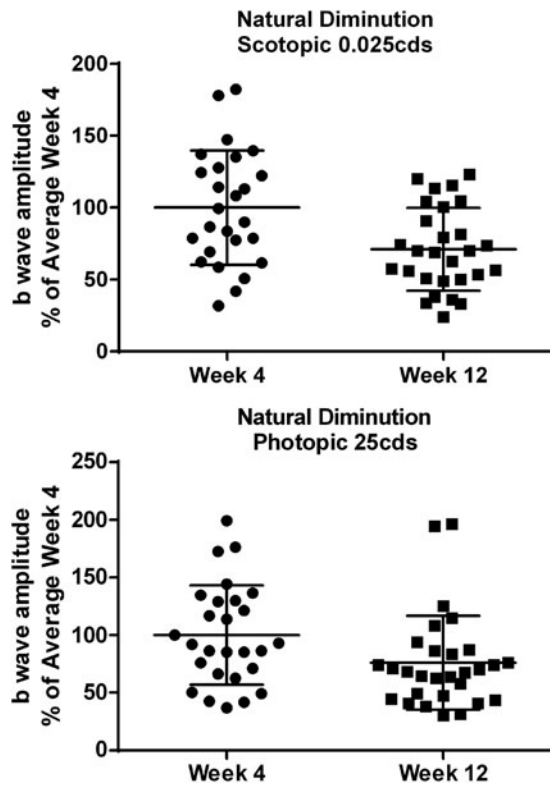
quence information from the MS/MS data were searched using Mascot Daemon by Matrix Science version 2.4.0 (Boston, MA) and the database searched against the full SwissProt database version 2017_06 (554,860 sequences; 198,649,153 residues). A decoy database was searched to determine the false discovery rate and peptides were filtered according to the results.

Statistical analyses

Hematology, coagulation, and clinical chemistry data were analyzed using analysis of variance and Dunnett's test. Organ weights and ERG were analyzed using analysis of variance and Tukey's multiple comparison test.

REFERENCES

- S1. Beltran WA, Cideciyan AV, Boye SE, et al. Optimization of retinal gene therapy for X-linked retinitis pigmentosa due to RPGR mutations. *Mol Ther* 2017;25:1866–1880.
- S2. Thomas DL, Wang L, Niamke J et al. Scalable recombinant adeno associated virus production using recombinant herpes simplex virus type 1 coinfection of suspension-adapted mammalian cells. *Hum Gene Ther* 2009;20:861–870.
- S3. Chulay JD, Ye GJ, Thomas DL, et al. Preclinical evaluation of a recombinant adeno-associated virus vector expressing human alpha-1 antitrypsin made using a recombinant herpes simplex virus production method. *Hum Gene Ther* 2011;22:155–165.
- S4. Ye GJ, Budzynski E, Sonnentag P, et al. Safety and biodistribution evaluation in CNGB3-deficient mice of rAAV2tYF-PR1.7-hCNGB3, a recombinant AAV vector for treatment of achromatopsia. *Hum Gene Ther Clin Dev* 2016;27:27–36.



Supplementary Figure 1. Natural diminution of Rd9 mouse electroretinography (ERG) response. Scotopic b-wave amplitudes to the low intensity stimulus (0.025 cds/m^2) and photopic response to the high intensity stimulus (25 cds/m^2) of the noninjected eyes were normalized to be the percentage change compared to the average of week 4, respectively. The percentage change was then plotted and statistically analyzed to compare the difference of ERG responses at week 4 and week 12, which was used to demonstrate the natural diminution of Rd9 ERG response. The mean and standard deviation of each distribution are provided.

HEK293 mRNA (1674) GGACGAGGAACGAGAGAAGGGCGAAAAGGATAAAAGGCCCGGGGAGATGGAACGACCTGGAGAGGGCGAAAAGAGCTGGCAGAGAAGGA
 Inj Ms mRNA (2027) GGACGAGGAACGAGAGAAGGGCGAAAAGGATAAAAGGCCCGGGGAGATGGAACGACCTGGAGAGGGCGAAAAGAGCTGGCAGAGAAGGA
 Ref hRPGRco (2679) GGACGAGGAACGAGAGAAGGGCGAAAAGGATAAAAGGCCCGGGGAGATGGAACGACCTGGAGAGGGCGAAAAGAGCTGGCAGAGAAGGA

HEK293 mRNA (1764) GGAATGGAAGAAAAGGGACGGCGAGGAACAGGAGCAGAAAAGAAAGGGAGCAGGGCCACCAGAAGGAGCGCAACCAGGAGATGGAAGAGGG
 Inj Ms mRNA (2117) GGAATGGAAGAAAAGGGACGGCGAGGAACAGGAGCAGAAAAGAAAGGGAGCAGGGCCACCAGAAGGAGCGCAACCAGGAGATGGAAGAGGG
 Ref hRPGRco (2769) GGAATGGAAGAAAAGGGACGGCGAGGAACAGGAGCAGAAAAGAAAGGGAGCAGGGCCACCAGAAGGAGCGCAACCAGGAGATGGAAGAGGG

HEK293 mRNA (1854) CGGCGAGGAAGAGCATGGCGAGGGGAGAAGAGGAAGAGGGCGATAGAGAAGAGGAAGAGGAAAAAGAGCGCAAGGGAAAGGAGGAAGGAGA
 Inj Ms mRNA (2207) CGGCGAGGAAGAGCATGGCGAGGGGAGAAGAGGAAGAGGGCGATAGAGAAGAGGAAGAGGAAAAAGAGCGCAAGGGAAAGGAGGAAGGAGA
 Ref hRPGRco (2859) CGGCGAGGAAGAGCATGGCGAGGGGAGAAGAGGAAGAGGGCGATAGAGAAGAGGAAGAGGAAAAAGAGCGCAAGGGAAAGGAGGAAGGAGA

HEK293 mRNA (1944) GGGCGAGGAAGTGGAAAGCGAGAGGGAAAAGGAGGAAGGAGAACGGAAGAAAAGAGGAAAGAGCCGGCAAAGAGGAAAAGGGCGAGGAAGA
 Inj Ms mRNA (2297) GGGCGAGGAAGTGGAAAGCGAGAGGGAAAAGGAGGAAGGAGAACGGAAGAAAAGAGGAAAGAGCCGGCAAAGAGGAAAAGGGCGAGGAAGA
 Ref hRPGRco (2949) GGGCGAGGAAGTGGAAAGCGAGAGGGAAAAGGAGGAAGGAGAACGGAAGAAAAGAGGAAAGAGCCGGCAAAGAGGAAAAGGGCGAGGAAGA

HEK293 mRNA (2034) GGGCGATCAGGGCGAAGGCGAGGAGGAAGAGACCAGGGCCCGGGGAAGAGAAAAGAGGAGGGAGGAGGTGGAGGGCGGAGAGGTCGA
 Inj Ms mRNA (2387) GGGCGATCAGGGCGAAGGCGAGGAGGAAGAGACCAGGGCCCGGGGAAGAGAAAAGAGGAGGGAGGAGGTGGAGGGCGGAGAGGTCGA
 Ref hRPGRco (3039) GGGCGATCAGGGCGAAGGCGAGGAGGAAGAGACCAGGGCCCGGGGAAGAGAAAAGAGGAGGGAGGAGGTGGAGGGCGGAGAGGTCGA

HEK293 mRNA (2124) AGAGGGAAAAGGGCGAGCGCAAGAGGAAGAGGAAGAGGGCGAGGGCGAGGAAGAAGAGGGCGAGGGGGAAGAAGAGGAGGAGAGGGCGA
 Inj Ms mRNA (2477) AGAGGGAAAAGGGCGAGCGCAAGAGGAAGAGGAAGAGGGCGAGGGCGAGGAAGAAGAGGGCGAGGGGGAAGAAGAGGAGGAGAGGGCGA
 Ref hRPGRco (3129) AGAGGGAAAAGGGCGAGCGCAAGAGGAAGAGGAAGAGGGCGAGGGCGAGGAAGAAGAGGGCGAGGGGGAAGAAGAGGAGGAGAGGGCGA

HEK293 mRNA (2214) AGAGGAAGAGGGGGAGGAAAAGGGCGAAGAGGAAGAGGAGGAAGGGGAGGAGGAAGAGGGGGAGGAGGGCGAGGGGGAAGGCCAGGA
 Inj Ms mRNA (2567) AGAGGAAGAGGGGGAGGAAAAGGGCGAAGAGGAAGAGGAGGAAGGGGAGGAGGAAGAGGGGGAGGAGGGCGAGGGGGAAGGCCAGGA
 Ref hRPGRco (3219) AGAGGAAGAGGGGGAGGAAAAGGGCGAAGAGGAAGAGGAGGAAGGGGAGGAGGAAGAGGGGGAGGAGGGCGAGGGGGAAGGCCAGGA

HEK293 mRNA (2304) GGAAGAAGGAGAGGGGGAAAGCGAAGAGGAAGGCCAGGGGGAAGGAGAGGAGGAAGAAGGGGAAGGCCAAGGCCAAGAGGAGGGAGAGG
 Inj Ms mRNA (2657) GGAAGAAGGAGAGGGGGAAAGCGAAGAGGAAGGCCAGGGGGAAGGAGAGGAGGAAGAAGGGGAAGGCCAAGGCCAAGAGGAGGGAGAGG
 Ref hRPGRco (3309) GGAAGAAGGAGAGGGGGAAAGCGAAGAGGAAGGCCAGGGGGAAGGAGAGGAGGAAGAAGGGGAAGGCCAAGGCCAAGAGGAGGGAGAGG

HEK293 mRNA (2394) AGAGGGGAGGAAGAGGAAGGAGAAGGGAAAGGGCGAGGAGGAAGGCCAAGAGGGAGAGGGGGAAGGCCAGGAAGAGGAAGGCCAGGGCGA
 Inj Ms mRNA (2747) AGAGGGGAGGAAGAGGAAGGAGAAGGGAAAGGGCGAGGAGGAAGGCCAAGAGGGAGAGGGGGAAGGCCAGGAAGAGGAAGGCCAGGGCGA
 Ref hRPGRco (3399) AGAGGGGAGGAAGAGGAAGGAGAAGGGAAAGGGCGAGGAGGAAGGCCAAGAGGGAGAGGGGGAAGGCCAGGAAGAGGAAGGCCAGGGCGA

HEK293 mRNA (2484) AGGAGAGGACGGCGAGGGCGAGGGAGAAGAGGAGGAAGGGGAATGGGAAGGCCAAGAAGAGGAAGGGCGAAGGCCAAGGCCAAGAAGAGGG
 Inj Ms mRNA (2837) AGGAGAGGACGGCGAGGGCGAGGGAGAAGAGGAGGAAGGGGAATGGGAAGGCCAAGAAGAGGAAGGGCGAAGGCCAAGGCCAAGAAGAGGG
 Ref hRPGRco (3489) AGGAGAGGACGGCGAGGGCGAGGGAGAAGAGGAGGAAGGGGAATGGGAAGGCCAAGAAGAGGAAGGGCGAAGGCCAAGGCCAAGAAGAGGG

HEK293 mRNA (2574) CGAAGGGGAGGGCGAGGAGGGCGAAGGCCAAGGGGAGGAAGAGGAAGGCCAAGGAGAAAGGCCAGGAAGAAGAGGGAGAGGAGGAAGGCCA
 Inj Ms mRNA (2927) CGAAGGGGAGGGCGAGGAGGGCGAAGGCCAAGGGGAGGAAGAGGAAGGCCAAGGAGAAAGGCCAGGAAGAAGAGGGAGAGGAGGAAGGCCA
 Ref hRPGRco (3579) CGAAGGGGAGGGCGAGGAGGGCGAAGGCCAAGGGGAGGAAGAGGAAGGCCAAGGAGAAAGGCCAGGAAGAAGAGGGAGAGGAGGAAGGCCA

HEK293 mRNA (2664) GGAGGAAGGAGAGGGGGAGGAGGAGGGAGAAGGCCAGGGCGAAGAAGAAGAAGAGGGAGAAGTGGAGGGCGAAGTTCGAGGGGGAGGAGGG
 Inj Ms mRNA (3017) GGAGGAAGGAGAGGGGGAGGAGGAGGGAGAAGGCCAGGGCGAAGAAGAAGAAGAGGGAGAAGTGGAGGGCGAAGTTCGAGGGGGAGGAGGG
 Ref hRPGRco (3669) GGAGGAAGGAGAGGGGGAGGAGGAGGGAGAAGGCCAGGGCGAAGAAGAAGAAGAGGGAGAAGTGGAGGGCGAAGTTCGAGGGGGAGGAGGG

HEK293 mRNA (2754) AGAAGGGGAAGGGGAGGAAGAAGAGGGCGAAGAAGAAGGCCAGGAAAGAGAAAAGAGGGAGAAGGCCAGGAAAACCGGAGAAAATAGGGA
 Inj Ms mRNA (3107) AGAAGGGGAAGGGGAGGAAAGAAGAGGGCGAAGAAGAAGGCCAGGAAAGAGAAAAGAGGGAGAAGGCCAGGAAAACCGGAGAAAATAGGGA
 Ref hRPGRco (3759) AGAAGGGGAAGGGGAGGAAAGAAGAGGGCGAAGAAGAAGGCCAGGAAAGAGAAAAGAGGGAGAAGGCCAGGAAAACCGGAGAAAATAGGGA

HEK293 mRNA (2844) AGAGGAGGAAGAGGAAGAGGGAAAGTACCAGGAGACAGCCGAAGAGG
 Inj Ms mRNA (3197) AGAGGAGGAAGAGGAAGAGGGAAAGTACCAGGAGACAGCCGAAGAGG
 Ref hRPGRco (3849) AGAGGAGGAAGAGGAAGAGGGAAAGTACCAGGAGACAGCCGAAGAGG

Supplementary Figure 2. Stability of *RPGRco* cDNA and mRNA. *RPGRco* mRNA extracted from HEK293 cells and mouse retina infected or injected with AAV2tYF-*RPGRco* vectors was sequenced after reverse transcription. All sequencing data were assembled based on the overlapping cDNA fragments using Vector NTI software to generate a consensus sequence that was compared to the human *RPGRco* reference sequence for analysis. mRNA fragment of *RPGRco* containing the high-frequency splicing region was demonstrated in this figure.

Supplementary Table S1. Ophthalmic examination findings for injected eyes

	<i>Group 1: Vehicle</i>		<i>Group 2: Low Dose</i>		<i>Group 3: High Dose</i>	
	<i>Week 4</i>	<i>Week 12</i>	<i>Week 4</i>	<i>Week 12</i>	<i>Week 4</i>	<i>Week 12</i>
Cornea lesion	9/10	10/10	9/9	10/10	10/10	9/9
Cornea opacity	9/10	0/10	6/9	0/10	10/10	0/9
Cornea edema	0/10	1/10	0/9	0/10	0/10	0/9
Synechia	6/10	2/10	2/9	3/10	1/10	1/9
Cataract	10/10	10/10	9/9	10/10	10/10	9/9
Vitreous in anterior chamber	2/10	1/10	1/9	0/10	0/10	1/9
Vitreous degeneration ^a	1/10	2/10	1/9	1/10	0/10	0/9
Mottling pigment	0/10	1/10	0/9	2/10	0/10	4/9
Retinal hemorrhage	0/10	0/10	1/9	0/10	0/10	0/9
Retinal vessel attenuation	0/10	0/10	0/9	1/10	0/10	3/9
Retinal detachment	0/10	0/10	1/9	0/10	0/10	0/9

^aVitreous opacity, strands, or liquefaction.

Supplementary Table S2. Incidence and severity of injection procedure–related microscopic findings: week 4 sacrifice

	<i>Group 1: Vehicle</i>		<i>Group 2: Low Dose</i>		<i>Group 3: High Dose</i>	
	<i>Males</i>	<i>Females</i>	<i>Males</i>	<i>Females</i>	<i>Males</i>	<i>Females</i>
Number Examined	6	4	5	5	5	5
Subretinal injection site						
Findings not present	4	1	2	2	1	4
Present	2	3	3	3	4	1
Degeneration, PR/ONL						
Findings not present	5	3	3	3	1	5
Minimal	0	0	1	2	0	0
Slight	0	0	1	0	3	0
Moderate	1	1	0	0	1	0
Pigmented cells, PR, retina						
Findings not present	4	1	2	3	1	4
Minimal	1	2	3	2	1	0
Slight	1	0	0	0	2	0
Moderate	0	1	0	0	1	1
Swollen, lens fibers						
Findings not present	6	3	5	5	5	3
Minimal	0	1	0	0	0	0
Slight	0	0	0	0	0	1
Moderate	0	0	0	0	0	1

PR, photoreceptor; ONL, outer nuclear layer.

Supplementary Table S3. Incidence and severity of injection procedure-related microscopic findings: week 12 sacrifice

	<i>Group 1: Vehicle</i>		<i>Group 2: Low Dose</i>		<i>Group 3: High Dose</i>	
	<i>Males</i>	<i>Females</i>	<i>Males</i>	<i>Females</i>	<i>Males</i>	<i>Females</i>
Number Examined	5	5	5	5	5	4
Subretinal injection site						
Findings not present	3	3	2	2	2	0
Present	2	2	3	3	3	4
Degeneration, ONL						
Findings not present	5	5	4	5	5	4
Marked	0	0	1	0	0	0
Degeneration, PR/ONL						
Findings not present	4	3	4	2	2	0
Minimal	1	0	0	2	0	1
Slight	0	2	1	1	2	3
Moderate	0	0	0	0	1	0
Pigmented cells, PR						
Findings not present	3	3	3	4	2	0
Minimal	2	0	1	1	2	3
Slight	0	2	1	0	1	1
Swollen, lens fibers						
Findings not present	5	4	4	5	5	4
Minimal	2	0	1	1	2	3
Moderate	0	0	1	0	0	0
Lens fibrosis						
Findings not present	5	5	4	5	5	4
Slight	0	0	1	0	0	0

Supplementary Table S4. Retinitis pigmentosa GTPase regulator immunolabeling in injected eyes

		<i>Group 1: Vehicle</i>		<i>Group 2: Low Dose</i>		<i>Group 3: High Dose</i>	
		<i>Males</i>	<i>Females</i>	<i>Males</i>	<i>Females</i>	<i>Males</i>	<i>Females</i>
Interim sacrifice (Week 4)	Number Examined	2	2	2	2	2	2
	RPGR immunolabeling						
	Slight	0	0	2	2	0	0
	Moderate	0	0	0	0	2	2
Terminal sacrifice (Week 12)	Number Examined	2	2	2	2	2	2
	RPGR immunolabeling						
	Slight	0	0	1	1	0	0
	Moderate	0	0	1	1	0	0
	Marked	0	0	0	0	2	2

RPGR, retinitis pigmentosa GTPase regulator.

Supplementary Table S5. Characterization of AAV2tYF-GRK1-RPGR drug product

<i>Test</i>	<i>Method</i>	<i>Result</i>
Vector concentration	Quantitative PCR	4.9×10^{12} vg/mL
Vector purity	SDS-PAGE	Pass (>90%)
Vector infectivity	TCID50	8.43×10^{11} TCID50 /mL
Endotoxin	Limulus amoebocyte lysis	Pass (<0.20 EU/ 1×10^{12} vg)
Sterility	Direct inoculation	Pass (no bacterial or fungal growth)
Mycoplasma	Broth and agar culture	Negative
Identity	Sanger Sequencing	Expected sequence
pH	pH meter	6.1

TCID50, tissue culture 50% infectious dose.